

Black Holes as Condensation Points of Fuzzy Dark Matter Cores

Curicaveri Palomares-Chávez,^{*} Iván Álvarez-Ríos,[†] and Francisco S. Guzmán[‡]

*Instituto de Física y Matemáticas, Universidad Michoacana de San Nicolás de Hidalgo. Edificio C-3,
Cd. Universitaria, 58040 Morelia, Michoacán, México.*

(Dated: December 23, 2024)

We simulate the formation of Fuzzy Dark Matter (FDM) cores in the presence of a Black Hole (BH) to explore whether BHs can serve as seeds for FDM core condensation. Our analysis is based on the core-condensation via the kinetic relaxation process for random initial conditions of the FDM. We show that in general the BH merges with pre-collapsed mini-clusters and once they share location the BH oscillates within the core. The condensation takes place around the black hole and the FDM acquires a density profile consistent with the density of the stationary solution of the FDM+BH eigenvalue problem in average. The central density of the resulting core depends on the mass of the BH, which due to its motion relative to the FDM cloud produces a smaller time-averaged densities for bigger BH masses, which lead to a new diversity of central FDM core densities. Our results indicate that BHs can indeed act as focal points for FDM core condensation. As a collateral result, for our analysis we revised the construction of stationary solutions of FDM+BH and found a phenomenological formula for the FDM density that can be used to fit FDM cores around BHs.

Keywords: dark matter – Bose condensates – black holes

Fuzzy Dark Matter (FDM) assumes dark matter is an ultralight boson with mass of order $10^{-23} - 10^{-21}$ eV, whose behavior differs from that of cold dark matter at galactic scales, in particular it promotes core formation and shows wave-like phenomena that produce a particular distribution of matter at galactic core and halo scales [1–4]. The structures formed by this particle are cores surrounded by envelopes with profiles similar to those of the CDM, being the core an essential fingerprint of the model determined from structure formation simulations (e.g. [5–10]).

Core formation has been studied in more detail at small scale simulations in basically two scenarios, one is the multi-merger of cores, for example in [6, 11–14] that leads to a simple construction of core-halo structures. Another approach uses the kinetic relaxation as explanation and simulation of core formation out of random initial conditions [15, 16]. These two methods help studying the core condensation process of bosonic configurations, their mass-growth and the envelope profile of their halos using small box simulations [17–20].

An essential ingredient introduced in FDM phenomenology is the presence of black holes and their behavior within FDM cores. For example, in [21, 22] the FDM core density profile properties are studied under various regimes of the boson gas and scenarios that include a black hole, in [23] the interaction of FDM and the BH is studied, in particular the dynamical friction and the drag of the wake behind the hole while moving, in [24] also the dynamical friction of FDM cores in BH is studied in merger scenarios, in [25] also the binary black hole merger moving inside FDM cores is studied

in the context of the final parsec problem of the merger. In gravitational wave related contexts, the binary black hole within FDM is studied to estimate the extraction of angular momentum due to dynamical effects of clumps of dark matter within the core [26]. In [27] the authors study the ejection of SMBHs due to the superposition of modes and the accumulation of random walk effects within FDM halos. Also in [28] the motion of a massive point particle in a FDM environment that includes its granules is studied, while in [24] the collision between an FDM core and a SMBH is analyzed. These studies consider the black hole to be Newtonian, and focus mainly in dynamic effects of moving black holes. In a relativistic context, the coexistence and phenomenology of black hole with ultralight bosonic dark matter has also been analyzed, for example in [29–32] various effects of black hole dynamics on the scalar field are studied, including dynamical friction, while in [33, 34] the analysis centers on the potential detection of ultralight dark matter via effects on gravitational wave phenomenology, including the case with self-interaction [35]. In cosmological scenarios, studies include for example the nucleation of scalar clouds [36].

In this work we study the effects of a BH during the FDM core-condensation, for which we follow the kinetic relaxation in [15, 16], that uses random initial conditions, so that the granularity of the FDM distribution develops in the presence of the BH since initial time. In our analysis we use a Newtonian description of the BH and add its gravitational potential to the Schrödinger-Poisson system of equations that rules the dynamics of the FDM+BH system, while we ignore the partial accretion of wave dark matter, which depends on the wavelength of wave-packets approaching the black hole, as demonstrated with full non-linear numerical relativity in [37, 38], as well as other non-linear accretion effects in non-symmetric scenarios [39].

^{*} curicaveri.palomares@umich.mx

[†] ivan.alvarez@umich.mx

[‡] francisco.s.guzman@umich.mx

The system of equations that rule the dynamics of the FDM+BH system is the following Schrödinger-Poisson system of equations:

$$i\hbar\partial_t\Psi = -\frac{\hbar^2}{2m}\nabla^2\Psi + mV\Psi, \quad (1)$$

$$\nabla^2V = 4\pi G(\rho_T - \bar{\rho}_T), \quad (2)$$

$$\ddot{\vec{x}}_{BH} = -\nabla V_{FDM}, \quad (3)$$

$$\nabla^2V_{FDM} = 4\pi G(\rho - \bar{\rho}), \quad (4)$$

where m is the boson mass, $\rho = m|\Psi|^2$ is the bosonic gas density, $\bar{\rho}$ its mean density, V is the gravitational potential due to the FDM and the BH, while V_{FDM} is the potential only due to the FDM; we approximate the BH with a density distribution $\rho_{BH} = M_{MH}\delta(\vec{x} - \vec{x}_{BH}) \simeq CM_{MH}e^{-|\vec{x}-\vec{x}_{BH}|^2/2\epsilon^2}$, which is an approximate Dirac delta distribution, where C is such that the integral of the distribution is the black hole mass M_{BH} ; the total density of the system is $\rho_T = \rho + \rho_{BH}$ and finally, \vec{x}_{BH} is the position of the black hole, that reacts to the gravity of the FDM.

In order to solve the SP system above, we use the transformations $t = t_0\tilde{t}$, $\vec{x} = x_0\tilde{\vec{x}}$, $V = V_0\tilde{V}$, $\Psi = \Psi_0\tilde{\Psi}$ and $\rho = \rho_0\tilde{\rho}$, where $t_0 = \frac{x_0^2 m}{\hbar}$, $V_0 = \left(\frac{\hbar}{m x_0}\right)$, $\Psi_0 = \frac{\hbar}{\sqrt{4\pi G m^3 x_0^2}}$, $\rho_0 = \frac{\hbar^2}{4\pi G m^2 x_0^4}$, that leave the SP system in dimensionless code units that only depend on the length scale parameter x_0 . We solve the dimensionless problem using the code CAFE-FDM [40], that implements a pseudo-spectral method to discretize spatial derivatives, an RK4 scheme for the evolution of the wave function, and the two Poisson equations are solved using the FFT method. All simulations are carried out in a periodic cubic domain of side L in code units, with resolution Δx . For the BH distribution we use $\epsilon = 0.1\Delta x$ because it gives similar results as in [24] for non-periodic domains, where a potential for the BH $V_{\bullet} = -\frac{GM_{BH}}{\sqrt{\max(r^2, \epsilon^2)}}$ is used within Schrödinger equation, but cannot be straightforwardly implemented in a periodic domain. As a test of our implementation, we evolve the eigen-solutions of the stationary FDM+BH configurations developed in [41] and verify they are stable.

Initial conditions. The kinetic relaxation leading to core condensation uses random initial conditions that eventually lead to the collapse of overdensities that in turn promote the bosonic gas condensation. The systematic study of this collapse process is understood from local simulations defined in [15, 16], where various distributions in the momentum domain are proposed, that give similar results. In our analysis we use a Gaussian distribution $\Psi(\vec{p}) = Ae^{-0.5p^2}e^{iS}$ in the momentum space, with S a random phase in the range $[0, 2\pi]$ at each point of the momentum space, where A is a normalization factor. In order to validate our methods and code, we run one of the simulation in [16], specifically a box of side $L = 18$, with resolution $\Delta x = L/128$ and total FDM

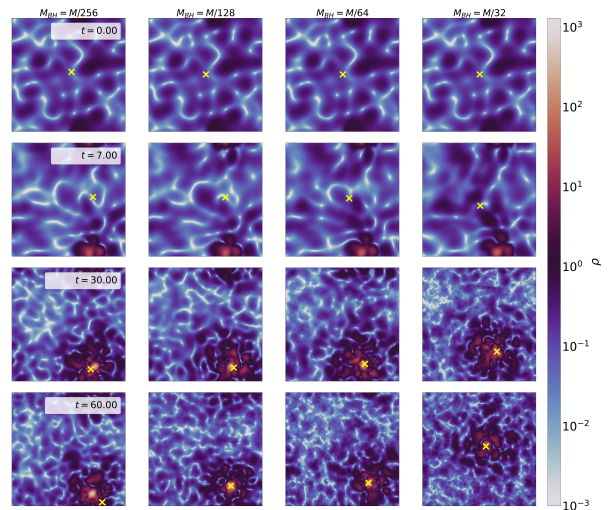


FIG. 1. Snapshots of the density projected on a plane that contains the position of the black hole and is parallel to the xy -plane of the numerical domain. The black hole position is represented with a yellow cross at different times for simulations with $M_{BH} = M/256, M/128, M/64$ and $M/32$. The evolution illustrates the formation of a minicluster near the bottom right corner. Later on the minicluster and the BH merge and start traveling together while the BH oscillates with respect to the core that can be better seen in the movies in the supplementary material. By $t \sim 60$ the FDM approaches condensation as seen in the analysis below.

mass $M_{FDM} = M = 1005.3$ and the results are shown in Appendix A as a test. We use these settings as default in our simulations involving BHs.

Simulations. We performed 32 simulations with the same type but different initial conditions for the FDM and various black hole masses $M_{BH} = M/256, M/128, M/64, M/32$, which lie within the range of masses used in studies of dynamical friction [23] and those of PBHs used for nucleation of axion stars in [36]. Different initial seeds for initial conditions lead to different evolutions of the FDM, however we illustrate the generic evolution of the system using the same particular seed to generate the random phase of FDM in Fourier space that in turn generates the initial conditions of the FDM, in the simulations with the four black hole masses. The evolution of the four cases is presented in Figure 1, that contains snapshots of the FDM density and the Black Hole position. At early times by $t \sim 7$ a minicluster forms near the bottom-right corner, later on this cluster merges with the black hole, following different trajectories for each black hole mass, and finally the condensation takes place at the black hole location. Animations of these simulations appear as Supplementary Material [42].

Condensation. In order to see if condensation happens, we monitor the evolution of ρ_{max} and the results are shown in Figure 2, where we notice that the conden-

sation takes place, the density grows with a power law of t starting after $t \sim 30$, which indicates the beginning of condensation, however later on the maximum density decreases or stabilizes instead of growing up as in the pure FDM scenario in [15, 16], that we use as test in Appendix A. The decrease of ρ_{max} is smaller for smaller black hole masses and can be understood in terms of the relative motion between the BH and the core, namely, the more massive the black hole is, the more FDM mass drags with it during relaxation. The black hole motion drags the FDM around and does not allow a quiet condensation, instead it is constantly revolving the FDM preventing the central density from growing, from becoming more compact. In this sense the Black Hole can act as an entity that decreases the final central FDM core density.

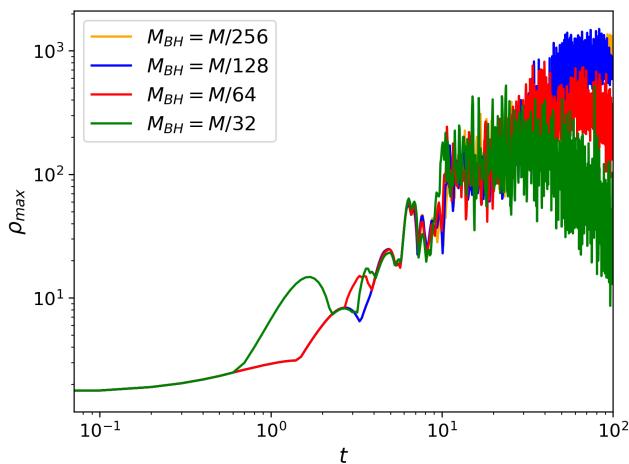


FIG. 2. Evolution of ρ_{max} for the various black hole masses $M_{BH} = M/256, M/128, M/64, M/32$. Notice that for the less massive BHs the density continues growing until $t \sim 60$ where it stabilizes. A difference between small BH masses and the case $M_{BH} = 0$ shown in Fig 7, is that ρ_{max} stabilizes with a BH, whereas it keeps growing when there is not BH in this time window, although as we will see below, the central density in average for the cases $M_{BH} = 0, M/256$ and $M/128$ are very similar. For the most massive BHs the maximum density decreases, which is an indication of the effects of the presence of the BH. For comparison of the evolution without BH see the simulations in Appendix A.

Relative motion. In Figure 3 we show the distance from the point of maximum density to the Black Hole, for the four values of M_{BH} . The non-linear behavior and the dynamics of the granularity lead to behavior that does not have a trend, since the motion of the black hole can be reheated differently since the different four mergers occur under different conditions, at different places and with different merging velocities, as can be seen in the animations.

Another part of the analysis is the velocity of the BH. In Figure 4 we show the x -component of the black hole's velocity, which shows the oscillatory behavior studied under smoother FDM distributions in [24]. Moreover, for

the cases $M_{BH} = M/128$ and $M/64$ the reheating pulses can be observed in the velocity as also described in [24]. Unlike in [24] the oscillations are less regular because we do not assume an initially smooth spherically symmetric core, but deal with the core resulting from the collapse of FDM, with all its granular multipolar components and time dependence, since the formation time.

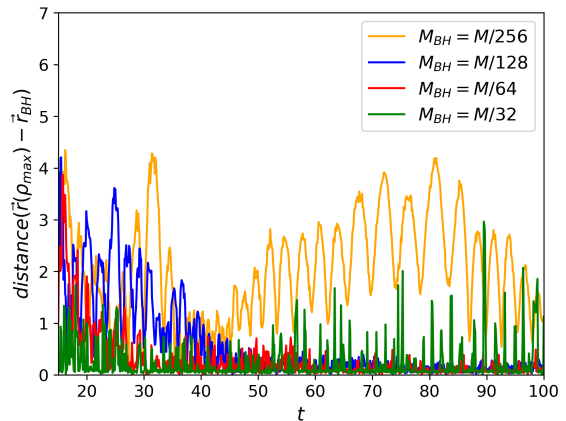


FIG. 3. Distance from the location of maximum FDM density to the black hole for $M_{BH} = M/256, M/128, M/64, M/32$ as function of time. There is no trend in the relative distance as function of M_{BH} , because the BH in each simulation catches up with the minicluster at different times, with different velocities, at different points within the FDM granularity, so that heating and friction act differently in the different cases.

Core fitting. Even though there is dynamics, we fit the resulting density profile of the FDM, not only at a fixed time but averaged over a time window using a phenomenological model for the density, that mimics the solution of the FDM-BH stationary eigen-problem in [41], as described in Appendix B; the FDM density fitting uses formulas (B3)-(B5). The result shows the possibility to fit the configuration with an equilibrium profile of the FDM-BH eigen-problem. The fittings are presented in Figure 5, that we obtain from averaging the density profile in the time window $t \in [70, 100]$, which is a lapse when, according to Fig. 2, the maximum density profile ends growing during condensation at least for the smallest black holes. Notice that the central core density is smaller for bigger BH mass, whereas the central core density converges to the case without BH when M_{BH} becomes smaller, in fact the cases $M_{BH} = M/256$ and $M/128$ have a profile similar already to that of the case $M_{BH} = 0$.

Summary of results. From our simulations we find that prior to the core condensation, miniclusters of FDM can form, that would collapse in themselves and condensate as shown in [15, 16] and in Appendix A. However the presence of the BH modifies such evolution and the minicluster merges with the black hole leading to the following effects. First, the FDM mass accommodates around the black hole, which shows how the black hole acts as an

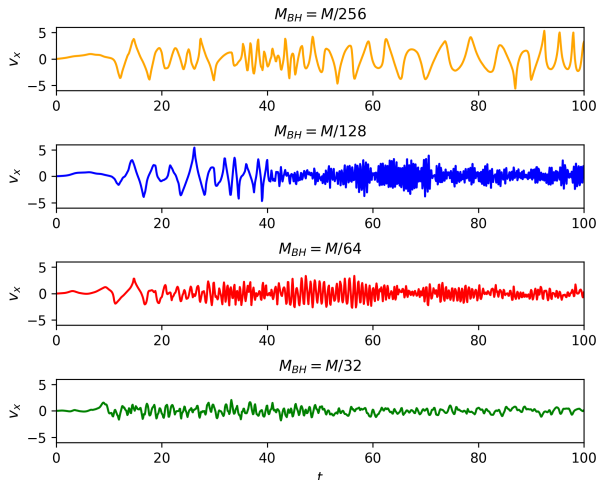


FIG. 4. The x -component of the BH velocity, for $M_{BH} = M/256, M/128, M/64, M/32$. These oscillations are consistent with those proposed in [24] for mergers of smooth cores and BHs. In our case the core has all its granules and time dependency since the beginning. Notice that for $M_{BH} = M/128, M/64$ the modulation of the velocity amplitude is consistent with the reheating of the BH motion. The behavior of the y and z -components of the velocity is similar. The animations in the Supplementary Material illustrate the whole picture of the process.

attraction point even for the smallest black hole mass case we used.

Second, the motion of the BH is oscillatory, a behavior found in [24] while studying the dynamical friction of FDM on black holes using formed spherically symmetric cores; here we showed that the oscillatory behavior happens even prior to core-condensation, within a non-spherically symmetric, time-dependent granular FDM distribution. The reheating of the BH motion due to the dynamics of the FDM can be observed as well.

Third, the analysis of ρ_{max} as function of time reveals that the FDM cloud starts condensing once it is around the BH, however its growth is affected by the presence of the BH motion. The motion of the BH within the core disperses the central density away, reducing the central averaged density of the FDM core. We find smaller central density of FDM for a bigger BH mass that drags the FDM around with its oscillatory motion.

Fourth, the solid angle and time averaged density of FDM around the black hole, can be modeled with the stationary spherically symmetric solutions of the FDM+BH

eigenvalue problem. The implication is that stationary solutions act like attractor solutions of FDM in the presence of a Black Hole.

In summary, our analysis shows that Black Holes act as condensation points where kinetic relaxation can take place. We consider that the influence of the black hole

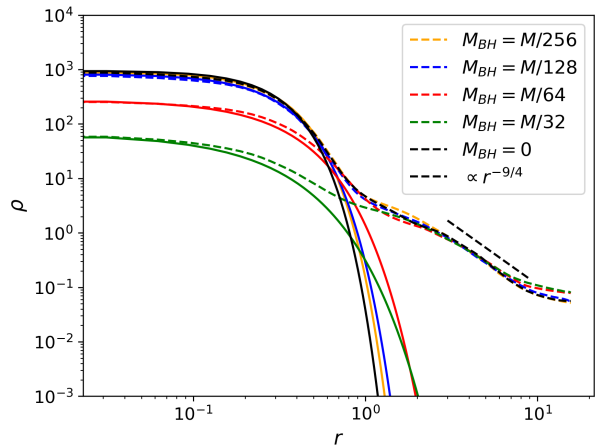


FIG. 5. Density fitting of the angularly and time averaged density of FDM around the BH, using the phenomenological formula (B3), for the simulations with $M_{BH} = M/256, M/128, M/64, M/32$. The time interval used to average density profiles is $t \in [70, 100]$. Notice that the more massive the black holes, the smaller the central core density, which is consistent with the notion of a Black Hole moving within the core while dragging FDM around and decreasing density, which is consistent with the results in Figure ???. We enclose the case for $M_{BH} = 0$ to show that when the mass of the BH approaches zero, the core approaches the case without BH.

in the galaxy formation context can lead to consistency checks of the FDM model, particularly in scenarios of galactic cores with supermassive black holes at their centers. The effects described in this work can lead to new detectable predictions that in turn should challenge the viability of the FDM model.

ACKNOWLEDGMENTS

We thank Pierre-Henri Chavanis for providing useful comments. Curicaveri Palomares and Iván Álvarez receive support from the CONAHCyT graduate scholarship program. This research is supported by grants CIC-UMSNH-4.9, Laboratorio Nacional de Cómputo de Alto Desempeño Grant No. 1-2024, CONAHCyT Ciencia de Frontera 2019 Grant No. Sinergias/304001.

[1] Pierre-Henri Chavanis, “Self-gravitating bose-einstein condensates,” in *Quantum Aspects of Black Holes*, edited

by Xavier Calmet (Springer International Publishing, Cham, 2015) pp. 151–194.

- [2] Jens C. Niemeyer, “Small-scale structure of fuzzy and axion-like dark matter,” *Progress in Particle and Nuclear Physics* **113**, 103787 (2020).
- [3] Lam Hui, “Wave dark matter,” *Annual Review of Astronomy and Astrophysics* **59**, 247–289 (2021).
- [4] Elisa G. M. Ferreira, “Ultra-Light Dark Matter,” arXiv e-prints, arXiv:2005.03254 (2020), arXiv:2005.03254 [astro-ph.CO].
- [5] Hsi-Yu Schive, Tzihong Chiueh, and Tom Broadhurst, “Cosmic Structure as the Quantum Interference of a Coherent Dark Wave,” *Nature Phys.* **10**, 496–499 (2014a), arXiv:1406.6586 [astro-ph.GA].
- [6] Philip Mocz, Mark Vogelsberger, Victor H. Robles, Jesús Zavala, Michael Boylan-Kolchin, Anastasia Fialkov, and Lars Hernquist, “Galaxy formation with Λ CDM turbulence and relaxation of idealized haloes,” *Mon. Not. Roy. Astron. Soc.* **471**, 4559–4570 (2017), arXiv:1705.05845 [astro-ph.CO].
- [7] Jan Veltmaat, Jens C. Niemeyer, and Bodo Schwabe, “Formation and structure of ultralight bosonic dark matter halos,” *Physical Review D* **98** (2018), 10.1103/physrevd.98.043509.
- [8] Philip Mocz, Anastasia Fialkov, Mark Vogelsberger, Fernando Becerra, Mustafa A. Amin, Sownak Bose, Michael Boylan-Kolchin, Pierre-Henri Chavanis, Lars Hernquist, Lachlan Lancaster, Federico Marinacci, Victor H. Robles, and Jesús Zavala, “First star-forming structures in fuzzy cosmic filaments,” *Phys. Rev. Lett.* **123**, 141301 (2019).
- [9] Simon May and Volker Springel, “Structure formation in large-volume cosmological simulations of fuzzy dark matter: impact of the non-linear dynamics,” *Monthly Notices of the Royal Astronomical Society* **506**, 2603–2618 (2021).
- [10] Bodo Schwabe and Jens C. Niemeyer, “Deep zoom-in simulation of a fuzzy dark matter galactic halo,” *Phys. Rev. Lett.* **128**, 181301 (2022).
- [11] Hsi-Yu Schive, Ming-Hsuan Liao, Tak-Pong Woo, Shing-Kwong Wong, Tzihong Chiueh, Tom Broadhurst, and W. Y. Pauchy Hwang, “Understanding the Core-Halo Relation of Quantum Wave Dark Matter from 3D Simulations,” *Phys. Rev. Lett.* **113**, 261302 (2014), arXiv:1407.7762 [astro-ph.GA].
- [12] Bodo Schwabe, Jens C. Niemeyer, and Jan F. Engels, “Simulations of solitonic core mergers in ultralight axion dark matter cosmologies,” *Phys. Rev. D* **94**, 043513 (2016), arXiv:1606.05151 [astro-ph.CO].
- [13] Iván Álvarez-Ríos, Francisco S. Guzmán, and Paul R. Shapiro, “Effect of boundary conditions on structure formation in fuzzy dark matter,” *Phys. Rev. D* **107**, 123524 (2023).
- [14] Iván Álvarez-Ríos and F. S. Guzmán, “Effects of boundary conditions on the core-halo mass scaling relation of fuzzy dark matter structures,” *Phys. Rev. D* **110**, 023530 (2024).
- [15] D. G. Levkov, A. G. Panin, and I. I. Tkachev, “Gravitational bose-einstein condensation in the kinetic regime,” *Phys. Rev. Lett.* **121**, 151301 (2018).
- [16] Jiajun Chen, Xiaolong Du, Erik W. Lentz, David J. E. Marsh, and Jens C. Niemeyer, “New insights into the formation and growth of boson stars in dark matter halos,” *Phys. Rev. D* **104**, 083022 (2021).
- [17] Benedikt Eggemeier and Jens C. Niemeyer, “Formation and mass growth of axion stars in axion miniclusters,” *Phys. Rev. D* **100**, 063528 (2019).
- [18] Jiajun Chen, Xiaolong Du, Mingzhen Zhou, Andrew Benson, and David J. E. Marsh, “Gravitational bose-einstein condensation of vector or hidden photon dark matter,” *Phys. Rev. D* **108**, 083021 (2023).
- [19] Kuldeep J. Purohit, Pravin Kumar Natwariya, Jitesh R. Bhatt, and Prashant K. Mehta, “Formation of a bose star in a rotating cloud,” *Astrophysics and Space Science* **368** (2023), 10.1007/s10509-023-04253-8.
- [20] Jiajun Chen and Hong-Yi Zhang, “Novel structures and collapse of solitons in nonminimally gravitating dark matter halos,” *Journal of Cosmology and Astroparticle Physics* **2024**, 005 (2024).
- [21] Pierre-Henri Chavanis, “Mass-radius relation of self-gravitating bose-einstein condensates with a central black hole,” *Eur. Phys. J. Plus* **134**, 352 (2019).
- [22] Pierre-Henri Chavanis, “Core mass-halo mass relation of bosonic and fermionic dark matter halos harboring a supermassive black hole,” *Physical Review D* **101** (2020), 10.1103/physrevd.101.063532.
- [23] Yourong Wang and Richard Easther, “Dynamical friction from ultralight dark matter,” *Phys. Rev. D* **105**, 063523 (2022).
- [24] Russell Boey, Yourong Wang, Emily Kendall, and Richard Easther, “Dynamical friction and black holes in ultralight dark matter solitons,” *Phys. Rev. D* **109**, 103526 (2024).
- [25] Hyeonmo Koo, Dongsu Bak, Inkyu Park, Sungwook E. Hong, and Jae-Weon Lee, “Final parsec problem of black hole mergers and ultralight dark matter,” *Physics Letters B* **856**, 138908 (2024).
- [26] Benjamin C. Bromley, Pearl Sandick, and Barmak Shams Es Haghi, “Supermassive black hole binaries in ultralight dark matter,” *Phys. Rev. D* **110**, 023517 (2024).
- [27] Amr A El-Zant, Zacharias Roupas, and Joseph Silk, “Ejection of supermassive black holes and implications for merger rates in fuzzy dark matter haloes,” *Monthly Notices of the Royal Astronomical Society* **499**, 2575–2586 (2020).
- [28] Lachlan Lancaster, Cara Giovanetti, Philip Mocz, Yonatan Kahn, Mariangela Lisanti, and David N. Spergel, “Dynamical friction in a fuzzy dark matter universe,” *Journal of Cosmology and Astroparticle Physics* **2020**, 001–001 (2020).
- [29] Vitor Cardoso, Taishi Ikeda, Rodrigo Vicente, and Miguel Zilhão, “Parasitic black holes: The swallowing of a fuzzy dark matter soliton,” *Physical Review D* **106** (2022), 10.1103/physrevd.106.1121302.
- [30] Dina Traykova, Rodrigo Vicente, Katy Clough, Thomas Helfer, Emanuele Berti, Pedro G. Ferreira, and Lam Hui, “Relativistic drag forces on black holes from scalar dark matter clouds of all sizes,” *Physical Review D* **108** (2023), 10.1103/physrevd.108.1121502.
- [31] Yuri Ravanal, Gabriel Gómez, and Normal Cruz, “Accretion of self-interacting scalar field dark matter onto a reissner-nordström black hole,” *Physical Review D* **108** (2023), 10.1103/physrevd.108.083004.
- [32] Alexis Boudon, Philippe Brax, and Patrick Valageas, “Supersonic friction of a black hole traversing a self-interacting scalar dark matter cloud,” *Phys. Rev. D* **108**, 103517 (2023).
- [33] Jamie Bamber, Josu C. Aurrekoetxea, Katy Clough, and Pedro G. Ferreira, “Black hole merger simulations in wave dark matter environments,” *Physical Review D* **107**

- (2023), 10.1103/physrevd.107.024035.
- [34] Josu C. Aurrekoetxea, Katy Clough, Jamie Bamber, and Pedro G. Ferreira, “Effect of wave dark matter on equal mass black hole mergers,” *Physical Review Letters* **132** (2024), 10.1103/physrevlett.132.211401.
- [35] Josu C. Aurrekoetxea, James Marsden, Katy Clough, and Pedro G. Ferreira, “Self-interacting scalar dark matter around binary black holes,” *Physical Review D* **110** (2024), 10.1103/physrevd.110.083011.
- [36] Mark P. Hertzberg, Enrico D. Schiappacasse, and Tsutomu T. Yanagida, “Axion star nucleation in dark minihalos around primordial black holes,” *Phys. Rev. D* **102**, 023013 (2020).
- [37] F. S. Guzmán and F. D. Lora-Clavijo, “Spherical nonlinear absorption of cosmological scalar fields onto a black hole,” *Phys. Rev. D* **85**, 024036 (2012).
- [38] F. G. Guzmán, I. Alvarez-Ríos, and J. A. González, “Frequency shift of light emitted from growing and shrinking black holes,” *Phys. Rev. D* **104**, 084014 (2021).
- [39] Vitor Cardoso, Taishi Ikeda, Rodrigo Vicente, and Miguel Zilhão, “Parasitic black holes: The swallowing of a fuzzy dark matter soliton,” *Phys. Rev. D* **106**, L121302 (2022).
- [40] Iván Álvarez-Ríos and Francisco S Guzmán, “Exploration of simple scenarios involving fuzzy dark matter cores and gas at local scales,” *Monthly Notices of the Royal Astronomical Society* **518**, 3838–3849 (2022).
- [41] Elliot Y Davies and Philip Mocz, “Fuzzy dark matter soliton cores around supermassive black holes,” *Monthly Notices of the Royal Astronomical Society* **492**, 5721–5729 (2020).
- [42] C. Palomares-Cávez, I. Alvarez-Rios, and F. S Guzmán, “Supplementary material,” https://drive.google.com/file/d/1AZ-3B37CXU_MYTjrmUswvD3FYN8uZkzU/view, accessed: 2024-12-18.
- [43] F. S. Guzmán and L. Arturo Ureña López, “Evolution of the schrödinger-newton system for a self-gravitating scalar field,” *Phys. Rev. D* **69**, 124033 (2004).

Appendix A: Pure FDM

As a test we show the core condensation without a BH in Figure 6, that contains snapshots of the density at different times on a plane that passes through the point of maximum density, where we can notice that between $t \approx 10$ and $t \approx 30$ a minicluster is formed and in later times the solitonic core gets condensed. Further analysis that evidences condensation appears in Figure 7 where the maximum density is plotted as function of time in units of the condensation time $\tau_g \propto \frac{v^6}{\bar{\rho}^2 \log(vL)}$ as found in [16], which for our simulation corresponds to $\tau_g \approx 7$. The results obtained are in agreement with the findings in [16] related to density growing with a power law of t .

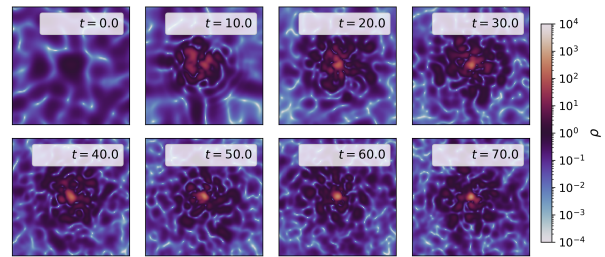


FIG. 6. Snapshots of the density on a plane that passes through the maximum density at various times. This simulation illustrates the condensation of an FDM core, resembling the results in [16].

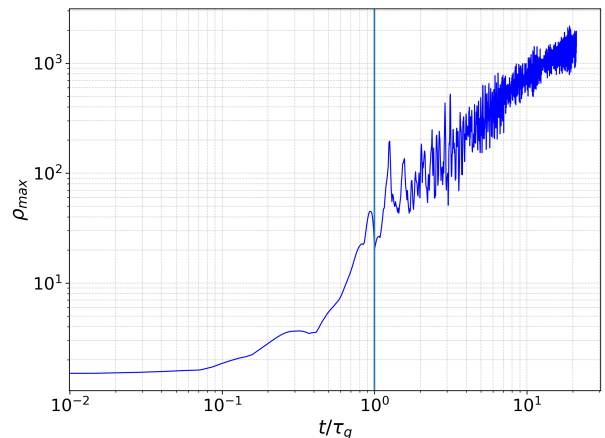


FIG. 7. Maximum density ρ_{max} in the numerical domain as function of time in units of τ_g . This plot illustrates the condensation process as shown in [15], which establishes the time scale τ_g for condensation, indicated with the vertical line.

Appendix B: Stationary Solutions

1. Solution of the FDM+BH eigenvalue problem

We construct stationary solutions for the FDM+BH problem following [41], whose equations are equivalent to the system (1)-(4) in the stationary regime

$$i\hbar\partial_t\Psi = -\frac{\hbar^2}{2m}\nabla^2\Psi + m_B(V + V_\bullet)\Psi, \quad (\text{B1})$$

$$\nabla^2V = 4\pi G(\rho - \bar{\rho}), \quad (\text{B2})$$

where $V_\bullet = -GM_{BH}/r$ is the gravitational potential due to a black hole of mass M_{BH} . The problem is solved in code units, spherical symmetry and harmonic time dependence of the parameter order $\Psi = \psi(r)e^{-i\omega t}$ with ψ a real function. These assumptions lead to an eigenvalue problem for the eigenvalue ω , provided isolation boundary conditions at infinity and regularity at the origin.

We note that this system exhibits invariance under the transformation $\{t', \Psi', x', V', \rho', M'_{BH}\} \rightarrow$

$\{\lambda^{-2}t, \lambda^2\Psi, \lambda^{-1}x, \lambda^2V, \lambda^4\rho, \lambda M_{BH}\}$, where λ is an arbitrary parameter. Now, for the construction of a phenomenological model of the FDM density we define the invariant $\alpha = M_{BH}^2/\psi_0$ under the λ -transformation, that allows one to parametrize the family of solutions of the eigenvalue problem. We note that in the limit $V_\bullet \gg V$ or equivalently $\alpha \gg 1$, the system reduces to the case of the hydrogen atom with ground state solution $\psi(r) = 2\left(\frac{1}{a_0}\right)^{3/2} e^{-r/a_0}$, being a_0 the Bohr radius. We thus propose a formula that in the limit of high α approaches the exponential solution

$$\rho(r, \alpha) = \rho_c e^{-\ln 2 \left(\frac{r}{r_c}\right)^\beta}, \quad (\text{B3})$$

where ρ_c is the central density, the core radius r_c is defined as the radius where the density decreases to the half of its central value and β is an α dependent function to be found.

In pure FDM scenarios, the ground state solution of the SP system (e.g. [43]) is difficult to use in phenomenological fitting of structures that are evolving within a simulation, then a practical formula for density was proposed to universally model FDM cores useful [5]. Here we do something analogous, since the solutions of the FDM+BH eigenvalue problem cannot be used to monitor the core formation around a black hole, thus we need a practical density profile that can be used during a simulation to fit the core density of the eigen-solution. To

do so, we search for a function that can fit the core properties, for example we choose for the core radius r_c the function

$$r_c = 1.3\rho_c^{-1/4} (1 + a_1 \ln(a_2\alpha + 1) + a_3\alpha^{a_4}), \quad (\text{B4})$$

with $a_1 = -0.25355872$, $a_2 = 0.46241994$, $a_3 = 0.0663722$ and $a_4 = 0.33407792$. Now, for every α there is a β , which according to the proposed formula (B3) fits the density of the solution of (B1)-(B2), this behavior can be described by the formula

$$\beta = \frac{b_1\alpha^{b_2}}{\alpha^{b_3} + b_4} + b_5, \quad (\text{B5})$$

with $b_1 = -1.08334305$, $b_2 = 0.77866182$, $b_3 = 0.81228993$, $b_4 = 6.72089826$ and $b_5 = 1.84588407$. In Figure 8 we plot the resulting eigenvalue of the system and compare the core radius and beta function against that of the eigen-solution of the eigen-problem (B1)-(B2). The asymptotic behavior of β corresponds to the limit $\beta \rightarrow 1$ when $\alpha \rightarrow \infty$.

In order to show these models work and that the solution of the eigenvalue problem can be fitted with these formulas, we show in Figure 8 the comparison between the density profiles resulting from the solution of the eigenvalue problem and that obtained with the formulas (B3), (B4) and (B5) for r_c and β above, for three different values of $\alpha = 0, 10, 100$.

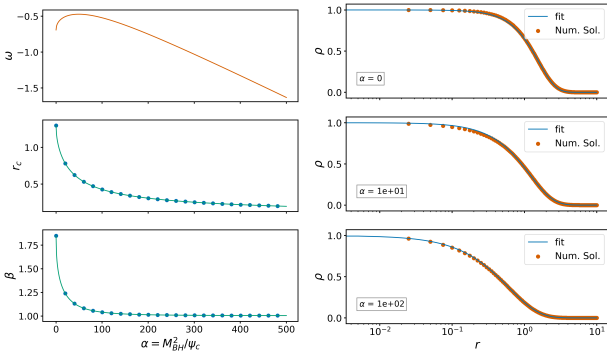


FIG. 8. (Left) At the top we show the eigenvalue ω as function of α . In the middle and bottom we show r_c and β as functions of α , where the dots correspond to genuine solutions of the eigenvalue problem and the continuous lines correspond to the values with our model formulas (B4) and (B5). (Right) Numerical solution of the eigenvalue problem, together with the density resulting from formulas (B3), (B4) and (B5) that model the solutions. In this plot we use $\alpha = 0, 10, 100$, in order to show that the model works fine for configurations with α orders of magnitude different.